Human Reproduction, pp. 1–11, 2018
doi:10.1093/humrep/dey365

human reproduction

ORIGINAL ARTICLE ***Reproductive biology***

Rab11a drives adhesion molecules to the surface of endometrial epithelial cells

Ruchi Kakar-Bhanot[1], Krupanshi Brahmbhatt[1], Bhagyashree Chauhan[1], R.R. Katkam[1], T. Bashir[2], H. Gawde[3], N. Mayadeo[4], U. K. Chaudhari[1], and Geetanjali Sachdeva[1,*]

[1]Primate Biology Laboratory, Indian Council of Medical Research-National Institute for Research in Reproductive Health (ICMR-NIRRH), Mumbai 400012, India [2]Molecular Immunology and Microbiology Laboratory, ICMR-NIRRH, Mumbai 400012, India [3]Genetic Research Centre, ICMR-NIRRH, Mumbai 400012, India [4]Department of Gynecology and Obstetrics, Seth G.S. Medical College and King Edward Memorial Hospital, Parel, Mumbai 400012, India

*Correspondence address. National Institute for Research in Reproductive Health (ICMR-NIRRH) J.M. Street, Parel, Mumbai 400012, India. Tel: +91-22-24192007; Fax: +91-22-24139412; E-mail: sachdevag@nirrh.res.in

Submitted on January 30, 2018; resubmitted on October 11, 2018; accepted on November 24, 2018

STUDY QUESTION: Is Rab11a GTPase, a regulator of intracellular trafficking, of significance in endometrial functions?

SUMMARY ANSWER: Rab11a is an important component of the cascades involved in equipping the endometrial epithelium (EE) with 'adhesiveness' and 'cohesiveness'.

WHAT IS KNOWN ALREADY: Cell adhesion molecules (CAMs) have been investigated extensively for modulation in their endometrial expression during the peri-implantation phase. However, the mechanisms by which CAMs are transported to the EE surface have not received the same attention. Rab11a facilitates transport of specific proteins to the plasma membrane in endothelial cells, fibroblasts, embryonic ectodermal cells, etc. However, its role in the transport of CAMs in EE remains unexplored.

STUDY DESIGN, SIZE, DURATION: *In-vitro* investigations were directed towards deciphering the role of Rab11a in trafficking of CAMs (integrins and E-cadherin) to the cell surface of Ishikawa, an EE cell line. Towards this, Rab11a stable knockdown (Rab-kd) and control clones of Ishikawa were generated. JAr (human trophoblastic cell line) cells were used to form multicellular spheroids. Pre-receptive ($n = 6$) and receptive ($n = 6$) phase endometrial tissues from women with proven fertility and receptive phase ($n = 6$) endometrial tissues from women with unexplained infertility were used.

PARTICIPANTS/MATERIALS, SETTING, METHODS: Rab-kd and control clones were used for *in-vitro* assays. Live cells were used for biotinylation, JAr spheroid assays, flow cytometry, trans-epithelial electrical resistance assays and wound-healing assays. Lysosome and Golgi membranes were isolated by ultracentrifugation. Confocal microscopy, immunoblotting, qRT-PCR and immunohistochemistry were employed for assessing the expression of Rab11a, integrins and E-cadherin.

MAIN RESULTS AND THE ROLE OF CHANCE: shRNA-mediated attenuation of Rab11a expression led to a significant ($P < 0.01$) decline in the surface localization of αVβ3 integrin. Cell surface protein extracts of Rab-kd clones showed a significant ($P < 0.05$) reduction in the levels of αV integrin. Further, a significant ($P < 0.01$) decrease was observed in the percent JAr spheroids attached to Rab-kd clones, compared to control clones. Rab-kd clones also showed a significant ($P < 0.001$) decline in the total levels of E-cadherin. This was caused neither by reduced transcription nor by increased lysosomal degradation. The role of Rab11a in maintaining the epithelial nature of the cells was evident by a significant increase in the migratory potential, presence of stress-fibres and a decrease in the trans-epithelial resistance in Rab-kd monolayers. Further, the levels of endometrial Rab11a and E-cadherin in the receptive phase were found to be significantly ($P < 0.05$) lower in women with unexplained infertility compared to that in fertile women. Taken together, these observations hint at a key role of Rab11a in the trafficking of αVβ3 integrin and maintenance of E-cadherin levels at the surface of EE cells.

LARGE-SCALE DATA: N/A.

LIMITATIONS, REASONS FOR CAUTION: The *in-vitro* setting of the study is a limitation. Further immunohistochemical localizations of Rab11a and CAMs were conducted on a limited number of human endometrial samples.

WIDER IMPLICATIONS OF THE FINDINGS: Rab11a-mediated trafficking of endometrial CAMs in EE cells can be explored further for its potential as a target for fertility regulation or infertility management.

STUDY FUNDING/COMPETING INTEREST(S): This study was funded by the Indian Council of Medical Research (ICMR), the Department of Science and Technology (DST), the Council of Scientific and Industrial Research (CSIR), Government of India. No competing interests are declared.

Key words: Rab11a / endometrium / receptivity / cell surface / integrin αVβ3 / E-cadherin / cell adhesion molecules

Introduction

An average sized human body is composed of ~3.72 × 10^{13} cells distributed in more than 20 different multicellular organs (Bianconi *et al.*, 2013). The multicellularity is believed to have co-evolved with the mechanisms for cell–cell adhesion and cell–extracellular matrix adhesion. The epithelium, an excellent example of multicellularity, executes several vital functions such as structural support, cohesion, protection against mechanical stress and barrier formation. All these functions critically rely on the cohesiveness of epithelial cells. Interestingly, tissues of different lineages can be distinguished by their epithelial layers with distinct protein repertoires which enable them to partake in cell/tissue-specific signalling, vectorial ion transport and secretion/absorption of specific biomolecules (Brown and Breton, 2000).

Endometrial epithelium (EE), a highly specialized multicellular layer, acts as a site for embryo anchorage. However, in humans, EE allows the embryo to implant only during the receptive phase in the menstrual cycle, thereby implying that the 'implantation-competence' is not an innate trait of EE. Akin to other epithelia, EE resists adhesion due to a polar organization of the plasma membrane with basolateral domains enriched with adhesive proteins and apical domains bereft of them. Paradoxically, it is the adhesion between the apical domains of endometrial and trophoblastic epithelia that sets the stage for initiation of implantation. Thus to become embryo-adhesive, EE requires modulation in its plasma membrane composition. EE plasma membrane undergoes several modifications during the receptive phase, including reduction in glycocalyx thickness and cell surface charge, loss of microvilli, flattening of the apical surface and differential expression of adhesion proteins (Murphy, 2004; Singh and Aplin, 2009). Further, receptivity is associated with loss of apical–basal polarity (Thie *et al.*, 1995; Aplin and Ruane, 2017). The protein repertoire of the EE plasma membrane is also rearranged during the receptive phase (Albers *et al.*, 1995; Denker, 1995; Buck *et al.*, 2012). However, sufficient efforts have not been made towards investigating the mechanisms involved in the trafficking of specific adhesion proteins to the EE plasma membrane.

Rab (Ras-related proteins in brain) proteins, members of the Ras superfamily of GTPases, have emerged as the master regulators of intracellular trafficking. Rab proteins oscillate between GTP-bound 'active' and GDP-bound 'inactive' states. Activated Rabs organize budding of vesicles containing a specific protein cargo to be transported from donor to acceptor compartment, cytoskeletal transport for vesicular movement between donor and acceptor compartments, and targeted docking and fusion of cargo-laden vesicles to the acceptor compartment (Stein *et al.*, 2003; Grosshans *et al.*, 2006). Temporal and spatial specificities to these events are rendered by interactions of Rabs with their specific downstream effectors (Vitale *et al.*, 1998; Barbero *et al.*, 2002; Vonderheit and Helenius, 2005).

Rab11 proteins are reported to play a crucial role in orchestration of the composition of plasma membrane (Roberts *et al.*, 2001; Lock and Stow, 2005). The present study investigates whether Rab11a, a member of Rab11 subfamily, plays a role in trafficking of CAMs (αv, β3 integrins and E-cadherin) in EE cells. Rab11a was selected on account of its placement at the intersection of exocytosis and endocytosis, and participation in both constitutive and regulated secretory pathways.

Materials and Methods

Cell line maintenance

Ishikawa cells (human endometrial adenocarcinoma cell line) (Sigma-Aldrich, USA) were grown in DMEM/Ham's F-12 medium (Sigma-Aldrich). STR (Supplementary Table SI) and karyotype analyses (Supplementary Fig. S1) of Ishikawa were carried out at Genetica DNA Laboratories (USA) and GRC, respectively. JAr cells (human choriocarcinoma cell line) (American Type Cell Culture, USA) were maintained in RPMI-1640 (Sigma-Aldrich). Media were supplemented with 10% foetal bovine serum (Gibco, USA), 100 units/ml penicillin and 100 µg/ml streptomycin (Gibco).

Human tissues

Pre-receptive ($n = 6$) and receptive ($n = 6$) phase endometrial tissues from proven fertile women and receptive phase ($n = 6$) samples from women with unexplained infertility were used for immunohistochemistry. The collection of human samples was approved by NIRRH Ethics Committee for Clinical Studies (181/2010) and written consent was obtained from the participants. Women in the fertile and infertile groups were aged 20–40 years with a history of regular menses, normal pelvic scan and hormonal profile, and no history of systemic or gynaecological diseases. These women were not using hormonal contraceptives. Women in the fertile group had carried at least one pregnancy beyond first trimester. Women in the infertile group had failed to conceive for more than a year and their spouses had normal semen parameters.

Antibodies

Details regarding the antibodies used in this study are presented in Supplementary Table SII.

Plasmids

TRC2-pLKO-puro vector encoding shRNA targeting the exonic region of human Rab11a (TRCN0000379577) was procured from Sigma-Aldrich.

pcDNA3.1 vector with the cDNA construct expressing dominant negative (S25N) mutant Rab11a protein was a gift from Dr Jim Norman, UK. TRC2-pLKO-puro vector without the shRNA construct and pcDNA3.1 vector without Rab11a cDNA were used as controls.

Generation of stable clones

For transient transfection, Ishikawa cells (1×10^5) were transfected with Rab11a cDNA construct expressing the mutant Rab11a protein (GDP-locked Rab11a) using Xtreme gene HP (Roche, Switzerland) for 48 h as per manufacturer's instructions.

Ishikawa cells, transfected with pLKO-puro plasmid construct (with or without Rab11a shRNAs) for 48 h, were further grown in puromycin supplemented media for seven days and those surviving due to integration of puromycin resistance gene in their genomes were sub-cultured individually. Protein lysates of 25 clones each from Rab11a shRNA and empty vector transfected cultures were prepared using lysis buffer (9 M Urea, 4% CHAPS, 40 mM Tris). Efficiency of Rab11a silencing was determined by immunoblotting and qRT-PCR (Supplementary Fig S2). Two different clones each for vector transfected (Control-1, Control-2) and Rab11a knockdown (Rab-kd-1, kd-2), derived from different colonies after stable transfection, were selected for further experiments.

RNA isolation, cDNA synthesis and qRT-PCR

Total RNA was isolated using RNeasy RNA isolation kit (Qiagen, Germany). RNA (2 µg) was converted to cDNA using High Capacity cDNA Reverse Transcription kit (Applied Biosystems, USA). cDNAs were amplified using specific Taqman primer-probes (Applied Biosystems) for Rab11a or E-cadherin and 18 S rRNA (endogenous control). The relative quantity (RQ) was calculated. Values were expressed as mean RQ ± S.E.M.

JAr spheroid attachment assay

JAr cells (2.5×10^5) in a 60 mm petri-dish (Nunc, Denmark) were incubated for 24 h on a rotary shaker for multicellular spheroid formation (John *et al.*, 1993). Spheroids (n = 40–50/well) were co-cultured for 2 h with confluent Rab-kd or control monolayers grown on coverslips. The coverslips were spun at 10 *g* for 5 min. Spheroids that remained bound after centrifugation were counted and expressed as percentage of the number of spheroids added initially.

Cytochemical localization

Cells (1.5×10^5), fixed with 3.7% *p*-formaldehyde in PBS for 25 min at RT, were incubated with primary antibodies overnight at 4°C and with secondary antibodies for 1 h at 37°C. Cells were stained with Phalloidin-594 for F-actin (Molecular Probes, Thermo Fisher Scientific) for 30 min. Nuclei were counter-stained with DAPI (4′,6-diamidino-2-phenylindole) (Roche). Cells were scanned using Carl Zeiss 510 Meta confocal laser scanning microscope (Germany).

Flow cytometry

Cells (1×10^5) harvested by controlled trypsin-EDTA treatment were incubated with anti-integrin αVβ3-alexa-488 antibody (0.5 µg) on ice for 30 min. The percentage of positive cells was calculated using FlowJo software.

Cell surface protein extraction

Cell surface proteins (CSP) were extracted using cell surface protein isolation kit (Thermo Fisher Scientific) as per the protocol (Bhagwat *et al.*, 2014). The eluted fraction had enrichment of CSPs as indicated by higher abundance of Integrin αV (Supplementary Fig S3A), compared to total protein lysate.

Wound healing assays

Cells (1×10^5/well) grown till 100% confluence were treated with 10 µg/ml Mitomycin-C (Sigma Aldrich) for 2 h. Wounds were created using a tip and monitored for the closure till 72 h. Images were captured at 0 and 72 h. Percentage wound closure was determined as follows: Area of wound at 72 h × 100/Area of wound at 0 h.

Trans-epithelial electrical resistance assay

Cells (3×10^5) were seeded on laminin (500 ng/ml) coated 0.4 µm inserts (Millipore Corporation, USA) (modified from Dewi *et al.*, 2004). To measure resistance, electrodes of a voltmeter (Millipore Corporation) were

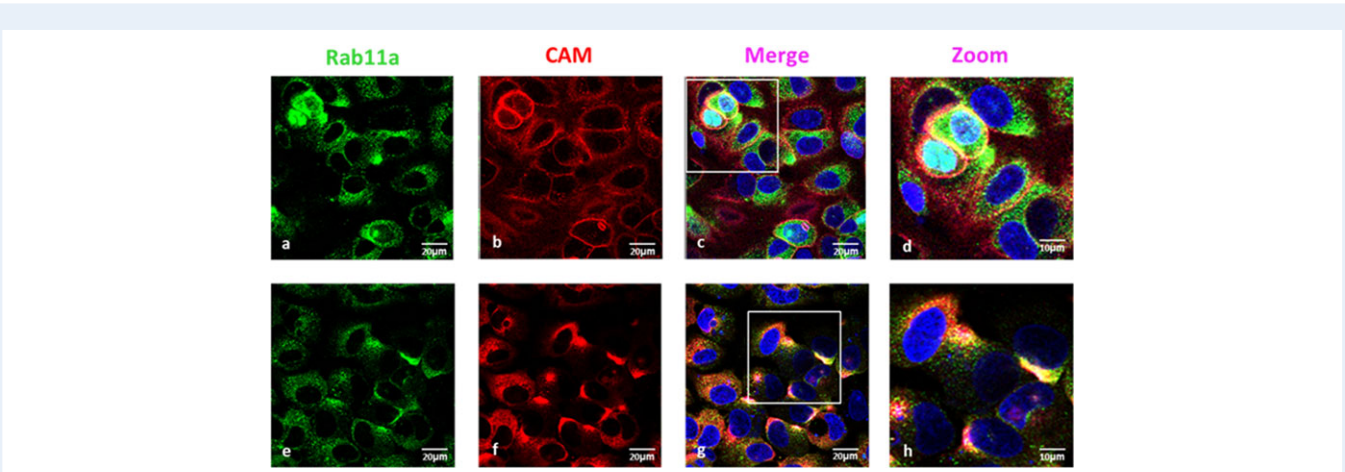

Figure 1 Co-localization of CAMs (Integrin αV or E-cadherin) with Rab11a in Ishikawa cells. αV (**b**–**d**) and E-cadherin (**f**–**h**) were detected using anti-mouse alexa fluor-594 (red) and Rab11a (**a**,**e**) was detected using anti-rabbit alexa fluor-488 (green). Images c and g (merge) represent co-localization of Rab11a with αV and E-cadherin respectively and images d and h represent the zoomed area (white box) of c and g panels, all with DAPI stained nuclei.

placed in the apical and basal compartments of the inserts. Percentage change in resistance was calculated as: Resistance value on Day $n \times 100$/ Resistance value on Day 1.

Isolation of lysosomal proteins

Lysosomes were isolated from cells (4.5×10^6) grown to 70–80% confluency, using Lysosome Enrichment kit (Thermo Fisher Scientific). Trypsinized cells were resuspended in Gradient dilution buffer (provided in the kit) and sonicated. Supernatants were collected by spinning suspensions at 500 *g* for 10 min and mixed with Optiprep (provided in the kit). The 15% Optiprep mix solution was overlaid on top of 17–30% discontinuous gradients of Optiprep mix. The lysosomal fraction was separated by ultracentrifugation at 145 000 *g* for 2 h at 4°C. The top-most layer containing the lysosomal fraction was isolated, washed with PBS and gradient dilution buffer at 18 000 *g* for 30 min at 4°C. Lysosomal pellet was resuspended in 1× gel loading dye. Lysosomal enrichment was checked by comparing LAMP1 levels in lysosomal and total protein extracts (Supplementary Fig. S3B).

Isolation of Golgi membrane extracts

Golgi membrane (GM) fractions were isolated as per the protocol (Balch *et al.*, 1984). Cells (4.5×10^6) grown to 70–80% confluency were scraped in breaking buffer (2.5 M sucrose, 10 mM Tris, pH 7.4). Cell pellets were diluted in five volumes of cold breaking buffer and homogenized till only nuclei were visible. Homogenates were diluted to 1.4 M sucrose supplemented with 100 mM disodium-EDTA (pH 8.0). Sucrose solutions (1.2 and 0.8 M) were sequentially overlaid on the homogenate. The gradient was ultracentrifuged at 90 000 *g* for 2.5 h at 4°C. Interphase between 0.8 and 1.2 M sucrose solution was collected and spun to obtain the GM pellet. GM protein enrichment was checked by comparing Mannosidase A1 (Man1 A1) levels in GM and total protein extracts (Supplementary Fig. S3C).

Immunoblotting

Immunoblotting was performed as per the protocol published previously (Bhutada *et al.*, 2014)

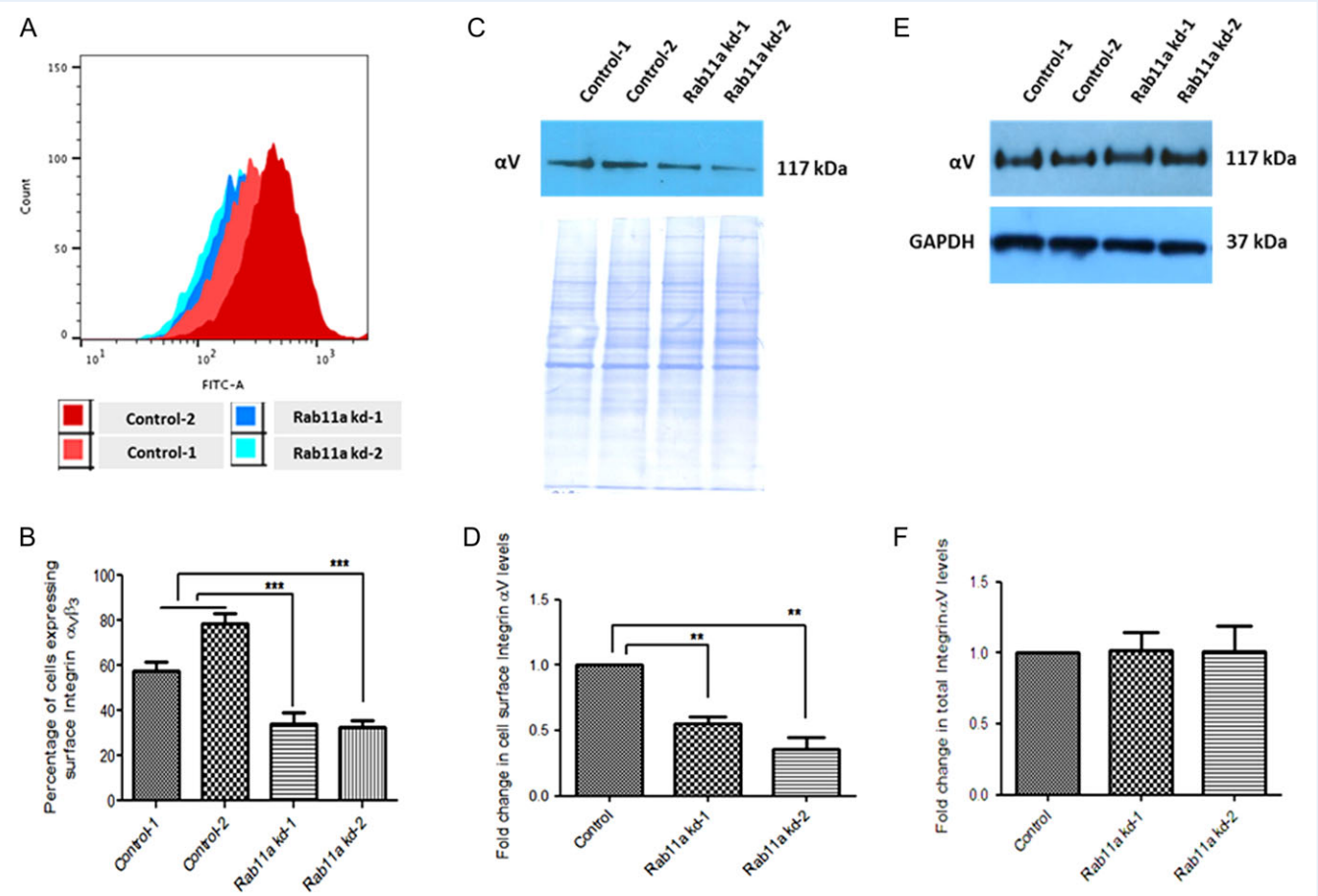

Figure 2 Effect of Rab11a knockdown on the cell surface and total integrin levels. Flow cytometric analysis (**A**, **B**) was done to enumerate the percent cells positive for surface αVβ3 in live, non-permeabilized Rab11a-kd and control clones. Three independent experiments were carried out with duplicates for each sample in each experiment. ***$P < 0.001$. Immunodetection of integrin αV in cell surface protein (CSP) extracts of control and Rab11a-kd clones and their respective total CSP loads are shown in **C**. (**E**) Displays immunodetection of αV and GAPDH in total protein lysates of control and Rab11a-kd clones. Densitometric analyses of the intensities of immunoreactive αV in the CSP fractions (**D**) or total lysates (**F**), normalized by total CSP load or GAPDH. Control taken as a calibrator, represents averaged ratios of intensities of cell surface αV to that of total CSP load or total αV to GAPDH in Control-1 and Control-2. **$P < 0.01$.

Immunohistochemistry

Endometrial sections were immunostained as per the protocol published previously (Bhutada *et al.*, 2014). Images of DPX mounted slides were captured using cellSens software (Olympus Corporation, Japan) and analysed using ImageJ software with IHC profiler plugin (https://sourceforge.net/projects/ihcprofiler/). Images were processed by deconvolution into three channels and analysed by pixel scores. Scores 4, 3, 2 and 1 allotted to intensities, determined by the software as high positive, positive, low positive and negative, respectively (Varghese *et al.*, 2014), were calculated for at least 10 random areas in each sample. Immunostaining score for each sample was calculated as the summed up score/total no. of images taken for each sample.

Statistical analyses

Statistical analyses were performed using SPSS software (V.25). Immunoblotting and Real-Time PCR data were analysed using student's unpaired *t*-test. Shapiro–Wilk test to assess normality of the data, one-way ANOVA with Bonferroni's post-hoc test for immunocytochemistry, spheroid attachment assay, flow cytometry, wound healing data and two-way ANOVA with Bonferroni's post hoc test for analysis of trans-epithelial electrical resistance (TEER) assay data were used. Mann–Whitney *U* test was employed for immunohistochemical data analysis. A value of $P < 0.05$ was considered statistically significant.

Results

Rab11a: subcellular location and co-localization with CAMs

Immunoreactive Rab11a was localized in the peri-nuclear region of Ishikawa cells (Fig. 1a and e). Further, Rab11a co-localized with integrin αV (Fig. 1b and c), and E-cadherin (Fig. 1f and g), suggesting that αV and E-cadherin are transported in Rab11a-positive vesicles. Cells transiently over-expressing mutant Rab11a showed reduced localization of integrin αV on the cell surface and also reduced adhesiveness to JAr spheroids (Supplementary Fig. S4), indicating that Rab11a activity is essential for the transport of αV integrin to the cell surface.

Effect of Rab11a depletion on cell surface localization of integrins

Two Rab11a stable knockdown clones (Rab kd-1 and 2) with more than 70% reduction at the protein level and two control clones (Supplementary Fig. S2B, C) were used for all subsequent *in-vitro* assays. Diminution of Rab11a expression did not alter the viability and proliferative capacity of Ishikawa cells (data not shown). Further, the reduction in Rab11a levels was not counterbalanced by an increase in Rab11b expression (Supplementary Fig. S2B).

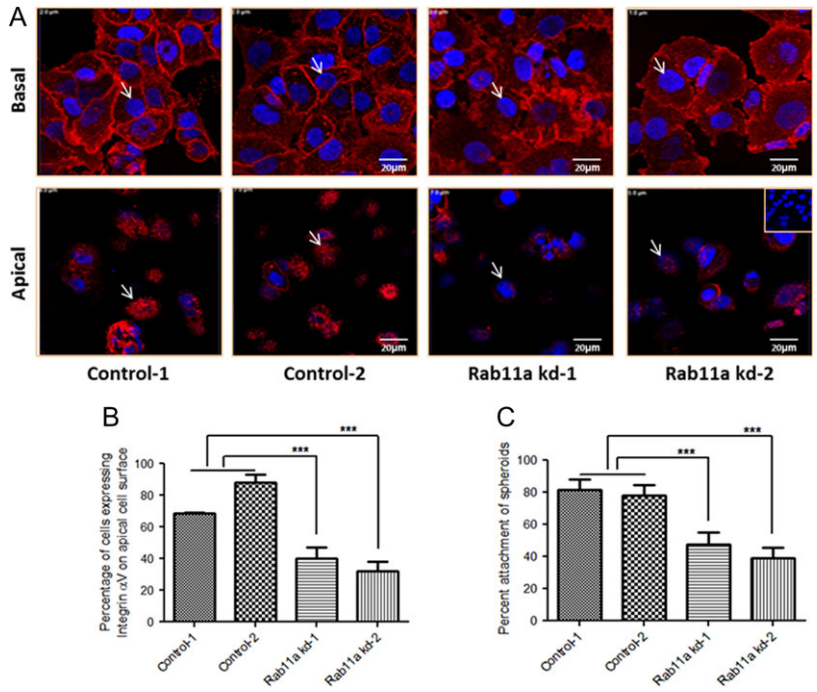

Figure 3 Effect of Rab11a knockdown on surface localization of Integrin αV and *in-vitro* adhesiveness to trophoblastic JAr spheroids. Rab11a knockdown (Rab11a kd-1, -2) and control clones (Control-1, -2) were immunostained for αV (**A**). The lower panels represent respective apical sections of the cells shown in the upper panel. Arrows represent the same cell in basal and apical sections. Negative control is shown in the inset. (**B**) Represents the percentage of cells displaying apical localization of αV ($n = 4$) ***$P < 0.001$. (**C**) Demonstrates the percent spheroids attached to Rab11a-kd and control clones ($n = 3$ with duplicates in each experiment). ***$P < 0.0001$.

Flow cytometry analysis using live non-permeabilized cells revealed a significant ($P < 0.01$) decrease in the percentage of surface αVβ3 immunopositive cells in Rab-kd clones, compared with control clones (Fig. 2A and B). CSP extracts of Rab-kd clones, compared to that of control clones, also showed lower abundance ($P < 0.05$) of integrin αV (Fig. 2C and D) and β3 (Supplementary Fig. S5). However, the total levels of αV and β3 did not differ significantly in Rab-kd and control clones (Supplementary Fig. 2E and F; Fig. S5), indicating that Rab11a depletion interferes with the transport of αV and β3, not with their expression.

Next, immunofluorescent localization and optical sectioning were carried out to determine whether the reduction in the levels of cell-surface αVβ3 in Rab-kd clones had a polar pattern. Optical sections of control clones, compared to those of Rab-kd clones, showed higher number of cells displaying αV immunopositivity on the apical side (Fig. 3A and B). Collectively, these observations suggest that Rab11a regulates the transport of integrins to the surface in EE cells.

Adhesive potential of Rab11a-deficient clones

Live Rab11a-sufficient Ishikawa cells, pretreated with antibody against the extracellular domain of integrin αV, showed a significant ($P < 0.001$) reduction in the number of attached JAr spheroids, compared to the cells pretreated with mouse IgG (Supplementary Fig. S6). This reiterated the relevance of endometrial cell surface αV integrin in adhesion to trophoblastic cells.

Rab-kd clones with reduced apical localization of αVβ3 were expected to have aberrant adhesiveness to JAr spheroids. This indeed was the case as the percentage of total spheroids adhered to Rab-kd clones was significantly lower compared to control clones (Fig. 3C).

Effect of Rab11a depletion on E-cadherin levels and localization

Significantly ($P < 0.01$) reduced immunoreactive E-cadherin staining was observed on lateral membranes in Rab-kd clones compared with control clones (Fig. 4A and B). Also, a significant ($P < 0.001$) reduction in total E-cadherin levels was detected in the total protein extracts of Rab-kd clones (Fig. 4C and D). However, transcript levels of E-cadherin did not differ in Rab-kd and control clones (Fig. 4E).

Effect of Rab11a depletion on E-cadherin levels in lysosomal and Golgi membrane extracts

Lysosomal and Golgi membrane fractions showed reduced levels of E-cadherin in Rab-kd clones, compared with control clones (Fig. 5). Interestingly, lysosomal levels of αV integrin did not differ in control and Rab-kd clones.

Effect of Rab11a depletion on migration and junctional permeability

In addition to E-cadherin, Claudin-1 (a tight junction protein) expression was found to be significantly ($P < 0.05$) down-regulated in Rab-kd

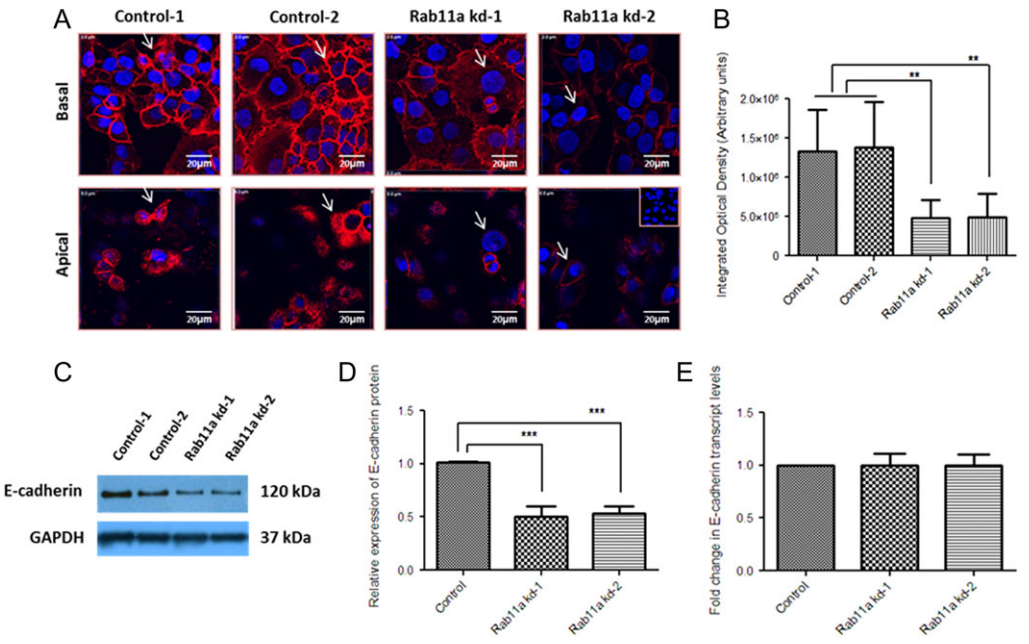

Figure 4 Effect of Rab11a knockdown on E-cadherin localization and expression. (**A**) Represents optical Z-sections displaying immunolocalization of E-cadherin on the basal and apical side. Negative control is shown in the inset. (**B**) Indicates the Integrated Optical Density of immunoreactive E-cadherin measured using ImageJ software, for 3D images reconstructed from optical sections. Intensity values were normalized by the area and number of cells analysed ($n = 3$). $^{**}P < 0.01$. (**C**) Shows a representative luminogram for E-cadherin and GAPDH levels. (**D**) Shows densitometric analysis of E-cadherin in total protein lysates of control and knockdown clones, normalized by GAPDH expression. Control represents averaged ratios of E-cadherin to GAPDH in Control-1 and Control-2 ($n = 3$). $^{***}P < 0.001$. **E** represents relative quantity of E-cadherin transcripts in Rab11-kd and control clones, normalized for their total RNA levels by 18S rRNA levels. The control, or calibrator, represents averaged values of ΔCt in Control-1 and Control-2 ($n = 3$ with each sample in triplicate).

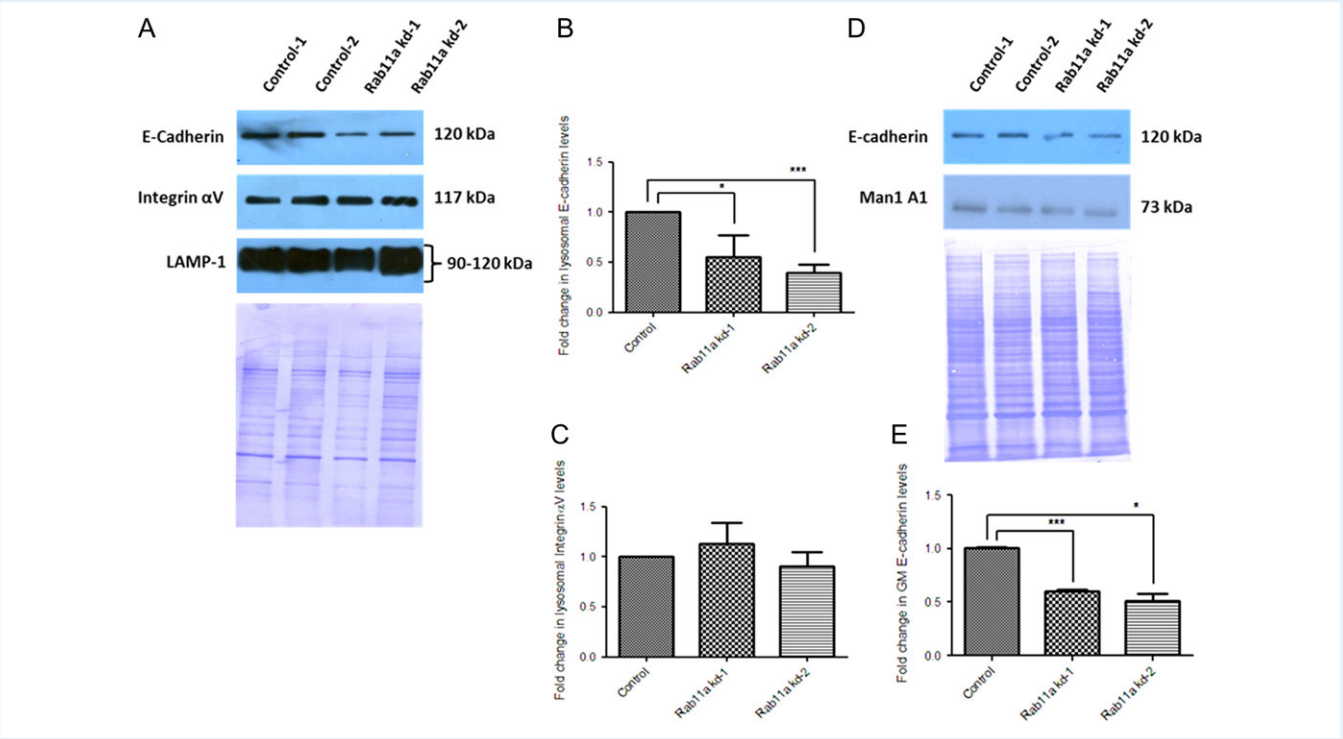

Figure 5 Effect of Rab11a knockdown on lysosomal proteins (LP) and Golgi Membrane (GM) levels of E-cadherin. (**A**) Displays immunoreactive E-cadherin, Integrin αV and LAMP1 in the LP extracts of control and Rab11a-kd clones. The protein blot stained with coomassie blue post-chemiluminescent detection depicts total LP load. (**B** and **C**) Demonstrate densitometric analyses of E-cadherin and αV levels respectively, in LP extracts of control and Rab11a-kd clones, normalized by LAMP1 expression ($n = 3$). *$P < 0.05$, ***$P < 0.001$. (**D**) Shows detection of E-cadherin and Mannosidase A1 (GM marker) in GM extracts from control and Rab11a-kd cells. Total GM protein load was visualized by staining the protein blot with coomassie blue post-chemiluminescent detection. (**E**) Represents densitometric analysis of E-cadherin in the GM extracts from control and Rab-kd clones, normalized by total GM protein load. *$P < 0.05$, ***$P < 0.001$.

clones (Supplementary Fig. S7). Next, we investigated whether reduction in the levels of E-cadherin and Claudin-1, due to Rab11a knockdown, modifies the migratory potential of Rab11a-deficient cells. In comparison to control clones, Rab11a-deficient clones displayed significantly ($P < 0.001$) higher migration (Fig. 6A and B). Further, these cells showed more stress-fibres in the cytoplasm and a loss of cortical organization of F-actin, indicating a rearrangement in actin cytoskeleton (Fig. 6C). Taken together, these observations hinted at a loss of the epithelial nature in Rab-kd clones. Rab kd-1 clone demonstrated significant ($P < 0.001$) reduction in the trans-epithelial electrical resistance on Days 4 and 5, compared to control clone-1, indicating formation of impaired tight junctions and loss of junctional integrity (Fig. 7). Rab kd-2 and Control-2 clones also showed a similar pattern (data not shown).

Rab11a, E-cadherin, Integrin αV and β3 immunolocalization in human endometrial samples

Rab11a immunoreactivity was predominantly localized in the apical regions of the cytoplasmic compartments of glandular (Supplementary Fig. S8a,b,e,f) and luminal (Supplementary Fig. S8c,d,g,h) epithelia and of the endometrial tissues from fertile women. Intensities of immunoreactive Rab11a did not differ significantly between the pre-receptive and receptive phases in fertile women (Supplementary Fig. S8).

Endometrial Rab11a expression in the receptive phase was found to be significantly ($P < 0.01$) reduced in infertile women, compared with control women (Fig. 8A). Interestingly, endometrial E-cadherin expression, predominantly detected in the lateral membrane, was also significantly ($P < 0.05$) lower in the infertile group (Fig. 8 and Supplementary Fig. S9). This pattern was also evident in the luminal epithelial compartment (Fig. 8C).

Among integrins, endometrial β3 levels appeared to be lower in infertile women, although the difference between fertile and infertile women failed to reach a statistical significance. β3 was found to be immunolocalised in both basal and apical cytoplasmic zones of epithelial cells, indicating its non-polar distribution in fertile women (Fig. 8A,d). However, in the infertile women, integrin β3 localization was majorly restricted to the basal side of epithelial cells (Fig. 8A,h).

Discussion

Acquisition of adhesiveness by the EE is a key element in the sequence of events contributing to uterine receptivity. Several cell adhesion molecules (CAMs) such as E-cadherin, ICAM-1, Trophinin, Basigin,

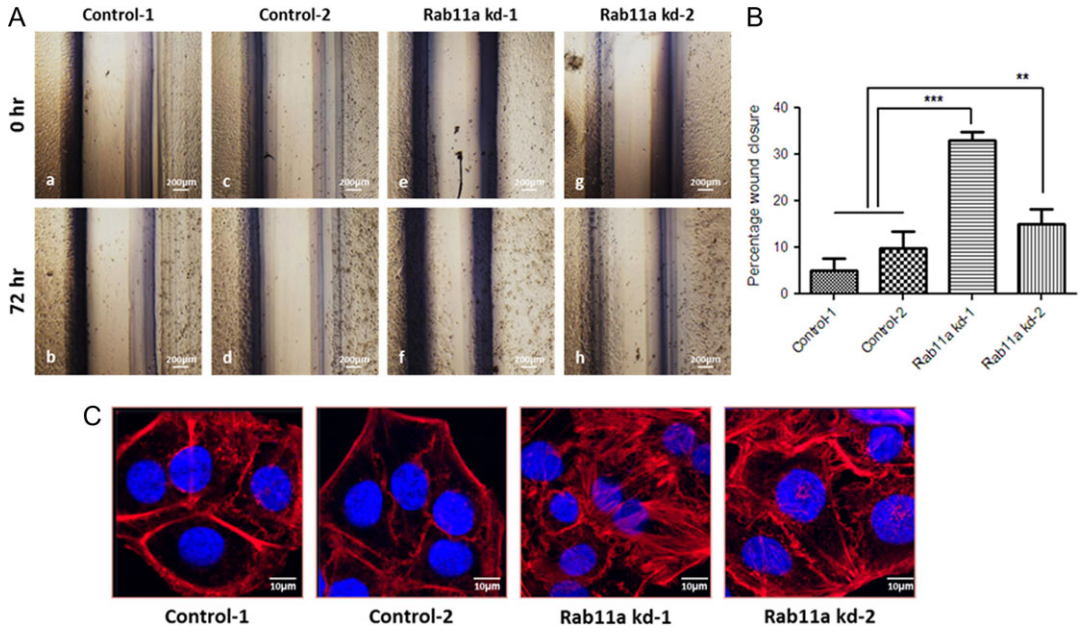

Figure 6 Effect of Rab11a knockdown on *in-vitro* migration and F-actin distribution. (**A**) Shows wounds at 0 h (a,c,e,g) and 72 h (b,d,f,h) in Rab11a-kd (e–h) and Control (a–d) clones. (**B**) Represents percentage wound closure after 72 h ($n = 3$ in duplicates). $^{**}P < 0.001$, $^{***}P < 0.0001$. (**C**) Shows cells stained with phalloidin to demonstrate F-actin distribution. Nuclei were counter-stained with DAPI.

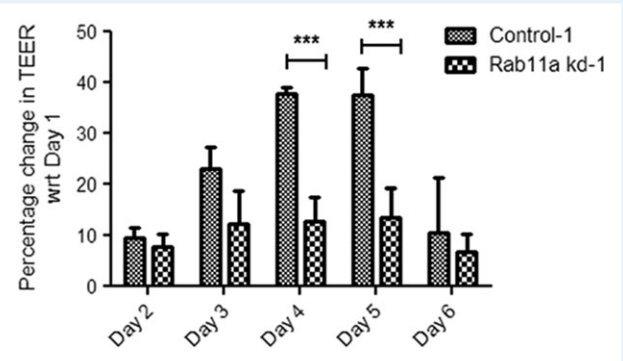

Figure 7 Trans-epithelial resistance of monolayers formed by Rab11a knockdown (Rab11a kd-1) and control (Control-1) clones. Percent change in resistance for control or knockdown clones from Days 2 to 6 was calculated from their respective resistance values recorded on Day 1 ($n = 3$). $^{***}P < 0.001$.

Integrins, etc. are differentially expressed in the EE during the receptive phase (Singh and Aplin, 2009). Strides have also been made to identify the endocrine and local cues which modulate the expression of CAMs during the receptive phase (Apparao *et al.*, 2002; Daftary *et al.*, 2002; Jha *et al.*, 2006; Lessey *et al.*, 2006; Bondza *et al.*, 2008; Rahnama *et al.*, 2009). However, the mechanisms underlying their trafficking to the EE plasma membrane have not been studied in depth. The present study attempts to gather insights into the contribution of intracellular trafficking to endometrial receptivity.

The present study is the first to demonstrate the role of Rab11a in the transport of integrins to the surface of EE cells. To model human EE, Ishikawa cells were used as they exhibit moderate apicobasal polarity and steroid responsiveness (Heneweer *et al.*, 2005). Akin to the cells over-expressing mutant Rab11 protein, Rab11a-deficient cells displayed reduced availability of αVβ3 on the surface without any change in the total αV levels. The ability of Rab11a-deficient clones to bind with trophoblastic spheroids was also impaired. Although Rab11a protein levels were depleted to a significant extent, 30–40% of the cells in Rab-kd clones retained immunopositivity for cell surface αVβ3. This can be attributed to either stochastic expression of Rab11 shRNA causing subclonal variegation or probable existence of alternate/additional mechanisms for αVβ3 localization to the cell surface. The data revealed no compensatory increase in Rab11b levels in Rab11a-kd clones. However, a possibility of Rab11c mediating αVβ3 transport to the cell surface cannot be negated. Irrespective of this, the study demonstrates that Rab11a expression and activity are important for integrin localization to the surface of EE cells.

Evidence exists to suggest that Rab11a is essential for transport of E-cadherin to the lateral membrane in MDCK (Lock and Stow, 2005) and endothelial (Yan *et al.*, 2016) cells. In endothelial cells, Rab11a depletion led to increased basal junctional permeability. The present study replicates these observations in EE cells as indicated by higher junctional permeability of Rab11a-kd cells. Claudin-1 levels were also reduced in Rab11a-kd cells. However, it is unclear whether this was a secondary effect due to loss of adherens junctions.

Interestingly, Rab11a deficiency caused a significant decline in the total levels of E-cadherin. This observation is in line with previous reports demonstrating an up-regulation in the E-cadherin levels on Rab11 overexpression in HT-29, a colon cancer cell line and co-overexpression of E-cadherin and Rab11 in colorectal tumours (Chung *et al.*, 2014). Thus, Rab11a appears to regulate cellular levels of E-

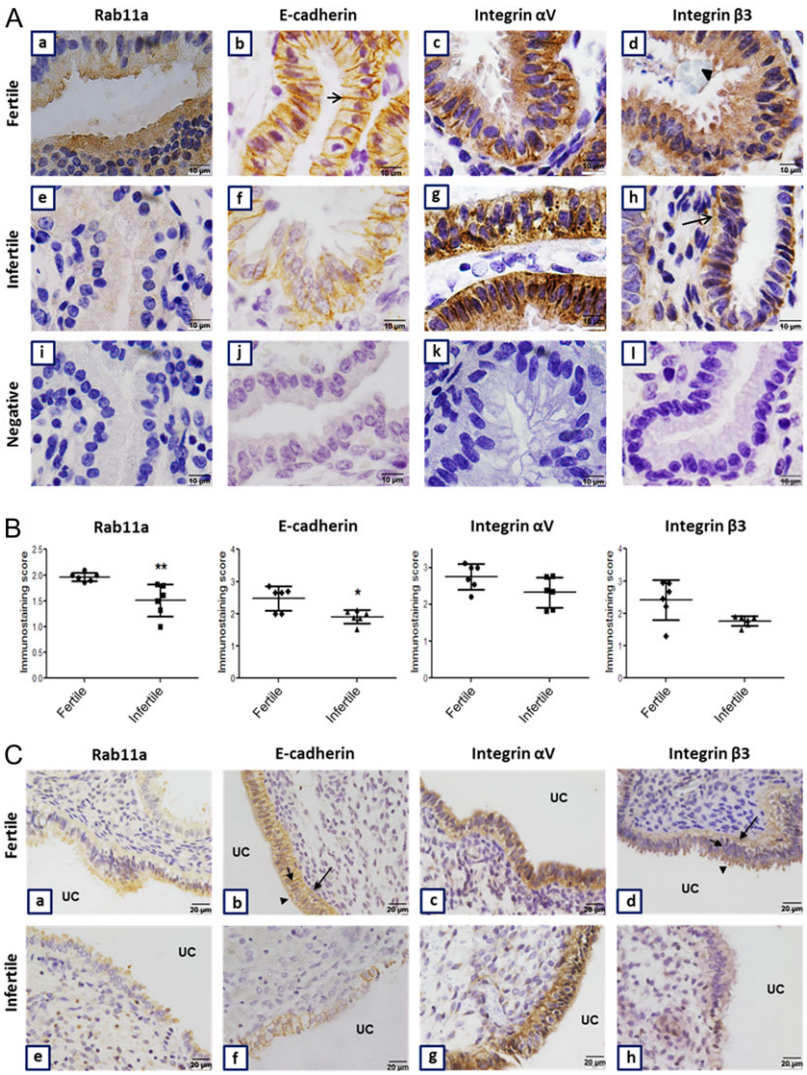

Figure 8 Endometrial immunolocalization of Rab11a, E-cadherin, Integrin αV and Integrin β3. (**A**) Shows a representative image to demonstrate immunolocalization of Rab11a (a,e), E-cadherin (b,f), αV (c,g) and β3 (d,h) in the receptive phase endometrial samples from women with proven fertility (a–d) and unexplained infertility (e–h). i-l are the sections where respective primary antibody was omitted. (**B**) Represents results of semi-quantitative analyses of intensities of immunoreactive Rab11a, E-cadherin, αV and β3 antigens. *$P < 0.05$, **$P < 0.01$. (**C**) Shows immunolocalisation of endometrial Rab11a (a,e), E-cadherin (b,f), αV (c,g) and β3 (d,h) in the luminal epithelium from fertile (a–d) and infertile (e–h) women. Arrows indicate immunopositivity on basal (big arrow) side, apical (arrowhead) side and lateral (small arrow) side. UC = uterine cavity.

cadherin. Rab11a is also reported to prevent lysosomal degradation of vascular E-cadherin protein in endothelial cells (Yan *et al.*, 2016). However, in our study, lysosomes were found to have significantly lower levels of E-cadherin in Rab11a-deficient cells. This ruled out the possibility of lysosomal degradation contributing to a reduction in the E-cadherin levels in Rab11a-deficient cells. Nonetheless, this indicates Rab11a functions are cell-context dependent. This was corroborated by another study demonstrating no effect of Rab11a depletion on E-cadherin localization in mouse embryos (Yu *et al.*, 2014).

A significant reduction observed in the E-cadherin protein expression following Rab11a knockdown was intriguing as Rab11a is not recognized for its role in regulating gene expression. The decline was neither caused by a modulation at the transcriptional level nor due to excessive lysosomal degradation. Interestingly, the Golgi membrane extracts of Rab11a-deficient cells also showed reduced levels of E-cadherin. There exists a possibility of Rab11a mediating trafficking of factors required for E-cadherin translation. Indeed, Rab11 is shown to be essential for efficient transport and translation of Oskar mRNA in Drosophila (Dollar *et al.*, 2002). It will be of interest to investigate the mechanism by which Rab11a regulates E-cadherin levels in EE cells.

Our *in-vitro* data suggested that Rab11a is important for deployment of integrins and E-cadherin to the surface of EE cells. This prompted us to assess whether Rab11a expression is modulated during the receptive phase. Our data did not reveal a significant change in endometrial Rab11a expression from pre-receptive to receptive phase. Nonetheless, considering that expression of endometrial αV and β3 is regulated by

progesterone (Lessey et al., 1996), it is likely that Rab11a functions assume more significance when αVβ3 integrins are in abundance.

This study, although conducted on a limited number of samples, demonstrated significantly lower levels of Rab11a in the EE of infertile women. Interestingly, E-cadherin levels were also found to be reduced in women with unexplained fertility. This observation is in agreement with previous studies demonstrating dysregulation in the endometrial E-cadherin expression in women with infertility and associated disorders (Poncelet et al., 2010; Makker et al., 2017). More investigations are warranted to establish whether Rab11a deficiency is indeed a cause of reduced E-cadherin levels in women with unexplained infertility.

In brief, the study demonstrates that Rab11a is essential for transport of integrins and maintenance of E-cadherin levels in EE cells. Aberrant localization and levels of CAMs due to Rab11a dysfunction may impair endometrial functions, through at least three modes, (i) by interfering with the adhesion between embryo and endometrium; (ii) by modifying or reducing the epithelial nature of endometrial cells and thereby depriving embryonic cells of a substratum to attach; or (iii) by disrupting the signalling cascades required for embryo–endometrial interactions. The study provides evidence for the first two possibilities. It will be interesting to study the signalling cascades that are disrupted due to impaired surface localization of CAMs.

Supplementary data

Supplementary data are available at *Human Reproduction* online.

Acknowledgements

The authors thank Dr B. Pathak for providing pLKO-puro vector and Dr Balasinor, Ms Reshma and Ms Shobha for confocal microscopy. Dr KVR Reddy is thanked for extending his facilities for TEER assays. The authors also thank Dr V. Bhor for providing LAMP1 antibody.

Authors' roles

R.K.B.: execution of experimental activities and article writing; K.B.: assistance in experiments; B.C.: immunohistochemical experiments; R. R.K.: characterization of tissue samples; T.B.: TEER assays; H.G.: karyotype analysis; N.M.: human sample collection; U.K.C: intellectual input; and G.S.: study conceptualization, data interpretation and article writing.

Funding

The Department of Science and Technology, Government of India is greatly acknowledged for financial support to R.R.K. R.K.B. sincerely thanks the Council of Scientific and Industrial Research (CSIR) and the Indian Council of Medical Research (ICMR) for providing fellowships to support her doctoral work.

Conflict of interest

None declared.

References

Albers A, Thie M, Hohn HP, Denker HW. Differential expression and localization of integrins and CD44 in the membrane domains of human uterine epithelial cells during the menstrual cycle. *Acta Anat (Basel)* 1995; **153**:12–19.

Aplin JD, Ruane PT. Embryo-epithelium interactions during implantation at a glance. *J Cell Sci* 2017;**130**:15–22.

Apparao KB, Lovely LP, Gui Y, Lininger RA, Lessey BA. Elevated endometrial androgen receptor expression in women with polycystic ovarian syndrome. *Biol Reprod* 2002;**66**:297–304.

Balch WE, Dunphy WG, Braell WA, Rothman JE. Reconstitution of the transport of protein between successive compartments of the Golgi measured by the coupled incorporation of N-acetylglucosamine. *Cell* 1984;**39**:405–416.

Barbero P, Bittova L, Pfeffer SR. Visualization of Rab9-mediated vesicle transport from endosomes to the trans-Golgi in living cells. *J Cell Biol* 2002;**156**:511–518.

Bhagwat SR, Redij T, Phalnikar K, Nayak S, Iyer S, Gadkar S, Chaudhari U, Kholkute SD, Sachdeva G. Cell surfactomes of two endometrial epithelial cell lines that differ in their adhesiveness to embryonic cells. *Mol Reprod Dev* 2014;**81**:326–340.

Bhutada S, Basak T, Savardekar L, Katkam RR, Jadhav G, Metkari SM, Chaudhari UK, Kumari D, Kholkute SD, Sengupta S *et al*. High mobility group box 1 (HMGB1) protein in human uterine fluid and its relevance in implantation. *Hum Reprod* 2014;**29**:763–780.

Bianconi E, Piovesan A, Facchin F, Beraudi A, Casadei R, Frabetti F, Vitale L, Pelleri MC, Tassani S, Piva F *et al*. An estimation of the number of cells in the human body. *Ann Hum Biol* 2013;**40**:463–471.

Bondza PK, Metz CN, Akoum A. Macrophage migration inhibitory factor up-regulates alpha(v)beta(3) integrin and vascular endothelial growth factor expression in endometrial adenocarcinoma cell line Ishikawa. *J Reprod Immunol* 2008;**77**:142–151.

Brown D, Breton S. Sorting proteins to their target membranes. *Kidney Int* 2000;**57**:816–824.

Buck VU, Windoffer R, Leube RE, Classen-Linke I. Redistribution of adhering junctions in human endometrial epithelial cells during the implantation window of the menstrual cycle. *Histochem Cell Biol* 2012;**137**:777–790.

Chung YC, Wei WC, Huang SH, Shih CM, Hsu CP, Chang KJ, Chao WT. Rab11 regulates E-cadherin expression and induces cell transformation in colorectal carcinoma. *BMC Cancer* 2014;**14**:587.

Daftary GS, Troy PJ, Bagot CN, Young SL, Taylor HS. Direct regulation of beta3-integrin subunit gene expression by HOXA10 in endometrial cells. *Mol Endocrinol* 2002;**16**:571–579.

Denker HW. Cell Biological views of embryo implantation (a review). *Turk J Med Sci* 1995:1–12.

Dewi BE, Takasaki T, Kurane I. In vitro assessment of human endothelial cell permeability: effects of inflammatory cytokines and dengue virus infection. *J Virol Methods* 2004;**121**:171–180.

Dollar G, Struckhoff E, Michaud J, Cohen RS. Rab11 polarization of the Drosophila oocyte: a novel link between membrane trafficking, microtubule organization, and oskar mRNA localization and translation. *Development* 2002;**129**:517–526.

Grosshans BL, Ortiz D, Novick P. Rabs and their effectors: achieving specificity in membrane traffic. *Proc Natl Acad Sci USA* 2006;**103**:11821–11827.

Heneweer C, Schmidt M, Denker HW, Thie M. Molecular mechanisms in uterine epithelium during trophoblast binding: the role of small GTPase RhoA in human uterine Ishikawa cells. *J Exp Clin Assist Reprod* 2005;**2**:4.

Jha RK, Titus S, Saxena D, Kumar PG, Laloraya M. Profiling of E-cadherin, beta-catenin and Ca(2+) in embryo-uterine interactions at implantation. *FEBS Lett* 2006;**580**:5653–5660.

John NJ, Linke M, Denker HW. Quantitation of human choriocarcinoma spheroid attachment to uterine epithelial cell monolayers. *In Vitro Cell Dev Biol Anim* 1993;**29**:461–468.

Lessey BA, Palomino WA, Apparao KB, Young SL, Lininger RA. Estrogen receptor-alpha (ER-alpha) and defects in uterine receptivity in women. *Reprod Biol Endocrinol* 2006;**4**:S9.

Lessey BA, Yeh I, Castelbaum AJ, Fritz MA, Ilesanmi AO, Korzeniowski P, Sun J, Chwalisz K. Endometrial progesterone receptors and markers of uterine receptivity in the window of implantation. *Fertil Steril* 1996;**65**:477–483.

Lock JG, Stow JL. Rab11 in recycling endosomes regulates the sorting and basolateral transport of E-cadherin. *Mol Biol Cell* 2005;**16**:1744–1755.

Makker A, Goel MM, Nigam D, Bhatia V, Mahdi AA, Das V, Pandey A. Endometrial expression of homeobox genes and cell adhesion molecules in infertile women with intramural fibroids during window of implantation. *Reprod Sci* 2017;**24**:435–444.

Murphy CR. Uterine receptivity and the plasma membrane transformation. *Cell Res* 2004;**14**:259–267.

Poncelet C, Cornelis F, Tepper M, Sauce E, Magan N, Wolf JP, Ziol M. Expression of E- and N-cadherin and CD44 in endometrium and hydrosalpinges from infertile women. *Fertil Steril* 2010;**94**:2909–2912.

Rahnama F, Thompson B, Steiner M, Shafiei F, Lobie PE, Mitchell MD. Epigenetic regulation of E-cadherin controls endometrial receptivity. *Endocrinology* 2009;**150**:1466–1472.

Roberts M, Barry S, Woods A, van der Sluijs P, Norman J. PDGF-regulated rab4-dependent recycling of alphavbeta3 integrin from early endosomes is necessary for cell adhesion and spreading. *Curr Biol* 2001;**11**:1392–1402.

Singh H, Aplin JD. Adhesion molecules in endometrial epithelium: tissue integrity and embryo implantation. *J Anat* 2009;**215**:3–13.

Stein MP, Dong J, Wandinger-Ness A. Rab proteins and endocytic trafficking: potential targets for therapeutic intervention. *Adv Drug Deliv Rev* 2003;**55**:1421–1437.

Thie M, Harrach-Ruprecht B, Sauer H, Fuchs P, Albers A, Denker HW. Cell adhesion to the apical pole of epithelium: a function of cell polarity. *Eur J Cell Biol* 1995;**66**:180–191.

Varghese F, Bukhari AB, Malhotra R, De A. IHC Profiler: an open source plugin for the quantitative evaluation and automated scoring of immunohistochemistry images of human tissue samples. *PLoS One* 2014; **5**:e96801.

Vitale G, Rybin V, Christoforidis S, Thornqvist P, McCaffrey M, Stenmark H, Zerial M. Distinct Rab-binding domains mediate the interaction of Rabaptin-5 with GTP-bound Rab4 and Rab5. *EMBO J* 1998;**17**:1941–1951.

Vonderheit A, Helenius A. Rab7 associates with early endosomes to mediate sorting and transport of Semliki forest virus to late endosomes. *PLoS Biol* 2005;**3**:e233.

Yan Z, Wang ZG, Segev N, Hu S, Minshall RD, Dull RO, Zhang M, Malik AB, Hu G. Rab11a mediates vascular endothelial-cadherin recycling and controls endothelial barrier function. *Arterioscler Thromb Vasc Biol* 2016; **36**:339–349.

Yu S, Yehia G, Wang J, Stypulkowski E, Sakamori R, Jiang P, Hernandez-Enriquez B, Tran TS, Bonder EM, Guo W *et al*. Global ablation of the mouse Rab11a gene impairs early embryogenesis and matrix metalloproteinase secretion. *J Biol Chem* 2014;**289**:32030–32043.

Human Reproduction, 2018
doi:10.1093/humrep/dey365

human reproduction

SUPPLEMENTARY DATA

Supplementary Table SI Short tandem repeat analysis of Ishikawa cells.

Sample reference number	Ishikawa (p.16) cell line (99040201)
LabCorpSpecNbr	79K90990
LabCorpCaseNbr	CX4004006
D3S1358	15, 16, 17, 18
TH01	8, 9, 10
D21S11	28
D18S51	13, 14, 19, 20
Penta E	11, 19, 20
D5S818	10, 11, 12
D13S317	9, 12, 13
D7S820	9, 10
D16S539	9
CSF1PO	11, 12
Penta D	10, 11
vWA	14, 16, 17, 18
D8S1179	11, 12, 16
TPOX	8
FGA	20, 21
AMEL	X
Mouse	*NA

*NA = no mouse DNA detected for this sample.

Supplementary Table SII **Details of the antibodies used in the study.**

Antibodies	Source (working concentration/dilution)			
	Immunoblotting	**Immunohistochemistry**	**Immunocytochemistry**	**Flow cytometry**
Rab11a	Abcam (0.5 μg/ml)	Santacruz Biotech (4 μg/ml)	Santacruz Biotech (0.02 μg/μl)	–
Integrin αV	Santacruz Biotech (0.2 μg/ml)	Santacruz Biotech (2.66 μg/ml)	–	–
Integrin β3	Abcam (0.477 μg/ml)	Santacruz Biotech (8 μg/ml)	Santacruz Biotech (2.66 μg/ml)	–
Integrin αVβ3 heterodimer—Alexa fluor 488	–	–	–	Santacruz Biotech and Novus Biologicals (0.5 μg)
E-cadherin	Abcam (1:100)	Abcam (1:175)	–	–
Glyceraldehyde 3-phosphate dehydrogenase	Calbiochem (0.33 μg/ml)	–	–	–
LAMP1	Cell Signalling Technology (1:2500)	–	–	–
Integrin αV (against extracellular domain)	–	–	Sigma Aldrich (0.013 μg/μl)	–
E-cadherin (against extracellular domain)	–	–	Abcam (1:25)	–
Mannosidase A1	Abclonal (1:500)	–	–	–
Secondary antibody tagged to Alexa fluor-488	–	–	Invitrogen (0.02 μg/μl)	–
Secondary antibody tagged to Alexa fluor-594	–	–	Invitrogen (0.02 μg/μl)	–
HRP tagged anti-mouse	Dako (0.13 μg/ml)	–	–	–
HRP tagged anti-rabbit	Dako (0.03 μg/ml)	–	–	–
Biotinylated anti-mouse and anti-rabbit	–	Vector Laboratories (1:100)	–	–
Mouse IgG	–	Merck Millipore (1:175)	Merck Millipore (0.013 μg/μl)	–
Rabbit IgG	–	Merck Millipore 4 μg/ml (for Rab11 experiment) 2.66 μg/ml (for Integrin αV experiment) 8 μg/ml (for Integrin β3 experiment)	–	–

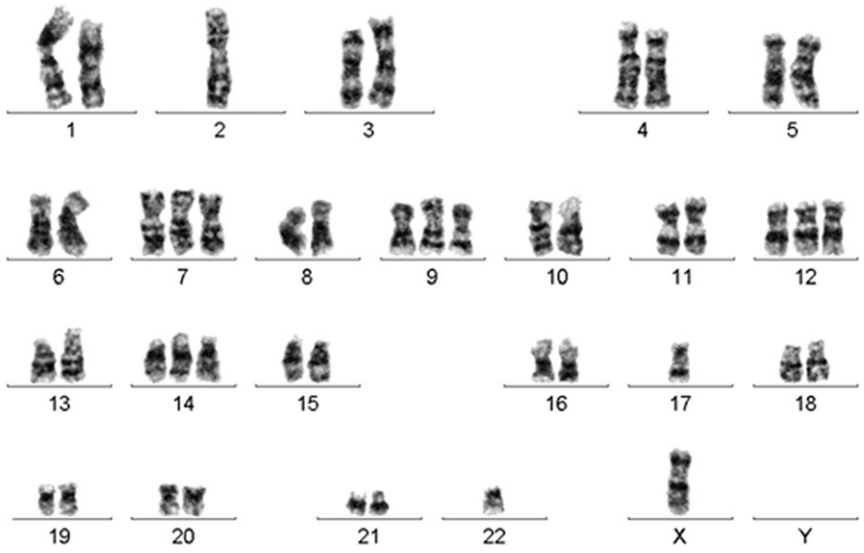

Supplementary Figure S1 **Karyotype analysis of Ishikawa cells**.

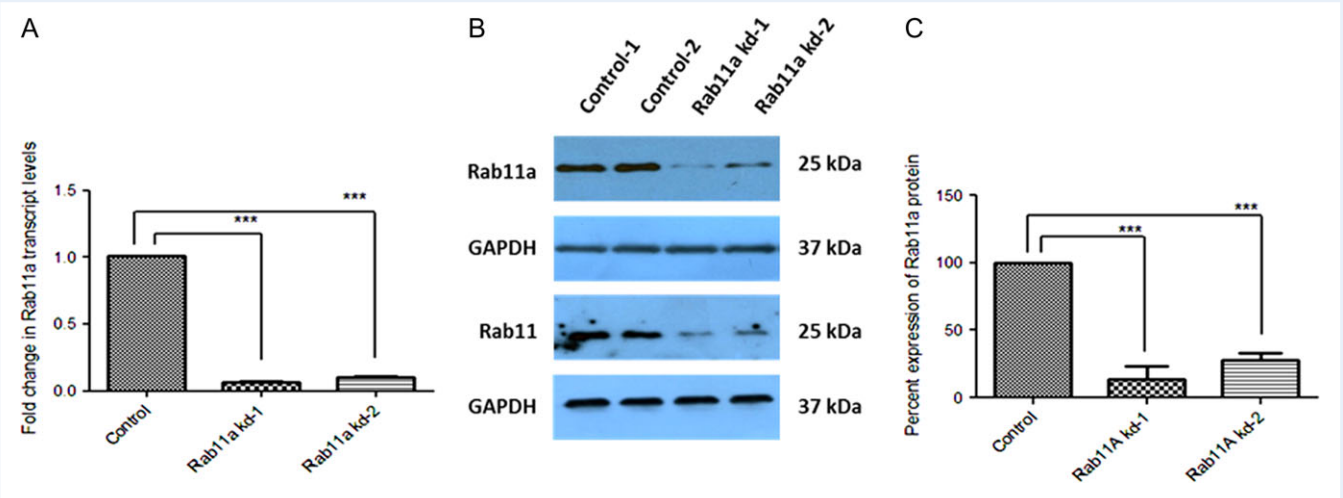

Supplementary Figure S2 Knockdown of Rab11a expression in Ishikawa cells. Rab11a expression in stable clones of Ishikawa expressing shRNA targeting Rab11a (Rab11a kd-1, kd-2) or empty vector (Control-1, Control-2). (**A**) Rab11a transcript levels in Rab11a-kd and control clones, normalized by 18 S rRNA levels. Control taken as a calibrator, represents averaged values of ΔCt in Control-1 and Control-2 ($n = 3$ with each sample in triplicate). ***$P < 0.0001$. (**B**) Immunodetection of Rab11a and Rab11 proteins in control and knockdown clones. (**C**) Densitometric analysis of immunoreactive Rab11a in protein lysates of Rab11a-kd and control clones, normalized by GAPDH expression. Control represents the averaged ratios of the intensities of Rab11a to that of GAPDH in Control-1 and Control-2 and is taken as Calibrator ($n = 3$). ***$P < 0.0001$.

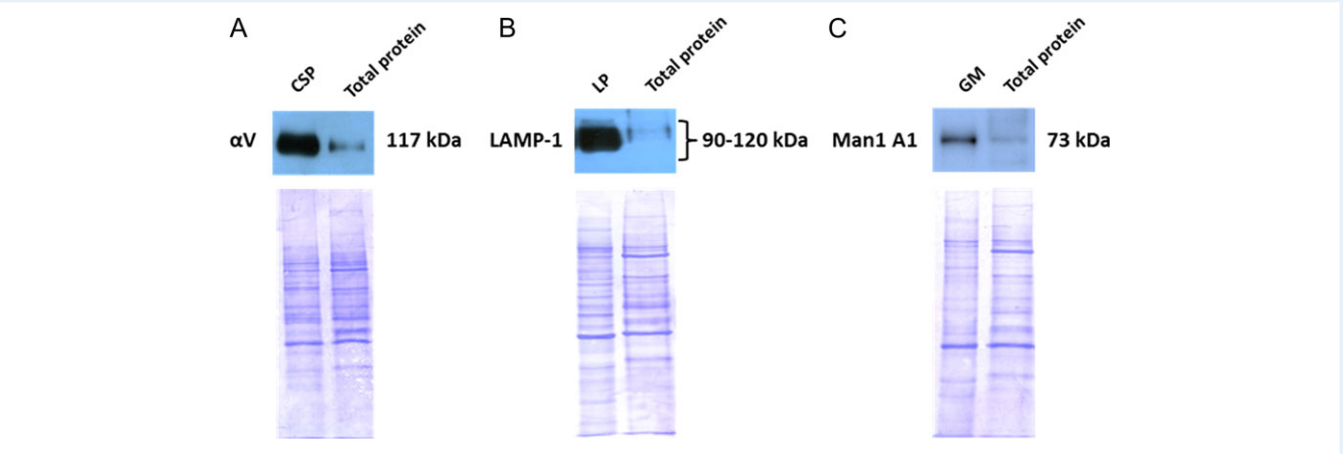

Supplementary Figure S3 **Isolation of cell surface proteins (CSP), lysosomal proteins (LP) and Golgi membrane (GM) proteins**. Enrichment of CSP (**A**), LP (**B**) and GM proteins (**C**) was confirmed by immunodetection of Integrin αV, LAMP1 and Mannosidase 1 (Man1 A1), respectively. Total protein load, as assessed by coomassie blue staining of blots with cell surface, lysosomal or Golgi membrane proteins, was used for normalization.

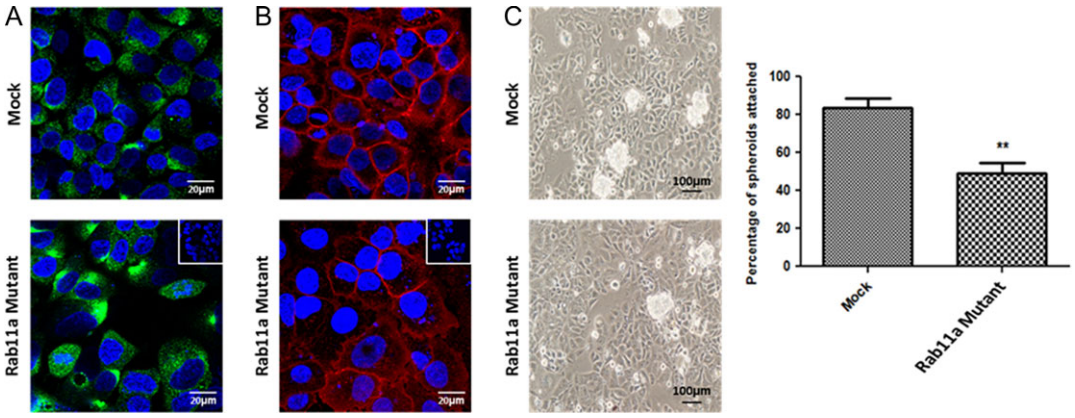

Supplementary Figure S4 Effect of mutant Rab11a on cell surface localization of integrin αV and spheroid attachment in Ishikawa cells. Panel A displays immunofluorescent detection of Rab11a protein (**A**) and Integrin αV (**B**) in cells transfected with empty vector (Mock) or vector encoding dominant negative Rab11a protein. Respective negative controls (where primary antibodies were omitted) are shown in the insets. (**C**) Displays *in-vitro* adhesion of transfected cells to trophoblastic JAr spheroids. Spheroid assays were repeated at three time points with each sample in duplicate ($n = 3$). $^{**}P < 0.01$.

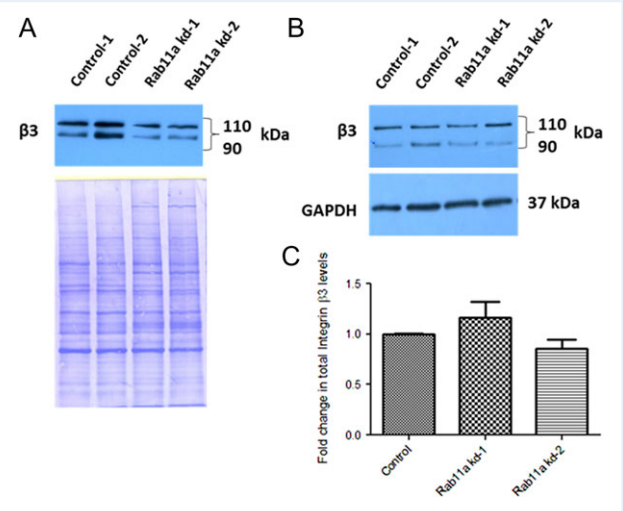

Supplementary Figure S5 Effect of Rab11a knockdown on cell surface and total levels of Integrin β3. Integrin β3 was immunodetected in cell surface protein extracts (**A**) and total protein lysates (**B**) of control and Rab11a-kd clones. Intensities of immunoreactive β3 were compared in Control and Rab11-kd clones, normalized by either total cell surface protein loads (for cell surface β3) or GAPDH (for total β3 levels).

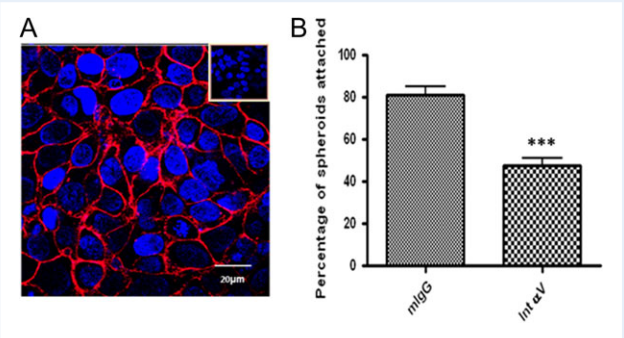

Supplementary Figure S6 Relevance of endometrial cell surface Integrin αV in adhesion to spheroids. (**A**) Shows binding of antibody against the extracellular domain of Integrin αV to the cell surface of non-permeabilized live cells. The inset shows cells stained with only secondary antibody. (**B**) Represents percent spheroids attached to Ishikawa cells, blocked with αV antibody or mouse IgG. $n = 3$ with each sample in duplicates. ***$P < 0.001$.

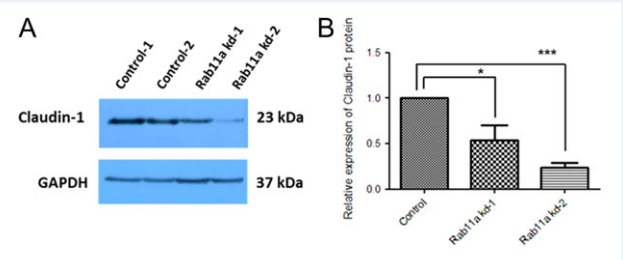

Supplementary Figure S7 Effect of Rab11a knockdown on Claudin-1, a tight-junction protein. (**A**) Shows immunoreactive Claudin-1 in the total protein lysates of Rab11a-kd and control clones. (**B**) Demonstrates densitometric analysis of the intensities of Claudin-1 protein in total protein lysates of control and Rab11a kd clones, normalized by GAPDH expression ($n = 3$). *$P < 0.05$, ***$P < 0.001$.

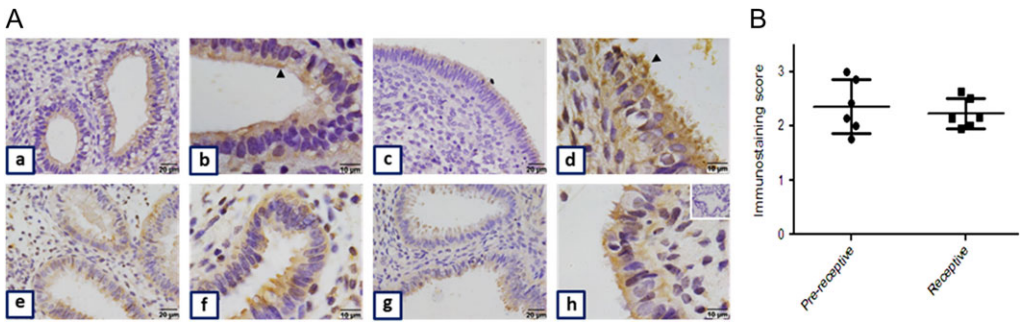

Supplementary Figure S8 Immunolocalization of Rab11a in pre-receptive and receptive phase endometrial samples from fertile women. (**A**) Depicts Rab11a in glandular epithelium (a,b,e,f) and luminal epithelium (c,d,g,h) of pre-receptive (a–d) and receptive (e–h) phase sections. Immunostaining in the apical side (arrowheads) in the glandular (b,f) and luminal epithelium (d,h) at a higher magnification is also shown. Negative control, where primary antibody was omitted, is shown in the inset. (**B**) Shows results of the semi-quantitative analysis of the intensities of immunoreactive Rab11a in the glandular epithelium of pre-receptive and receptive phase endometrial samples. $P > 0.05$.

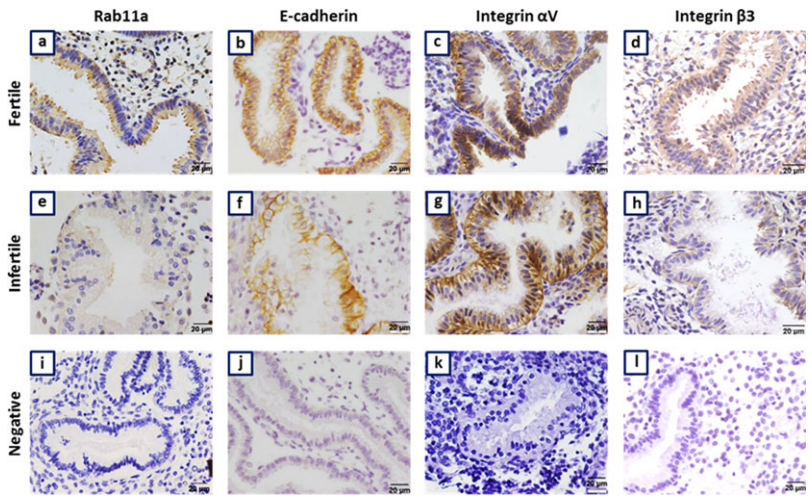

Supplementary Figure S9 Immunolocalization of endometrial Rab11a, E-cadherin, Integrin αV and Integrin β3. Representative images demonstrate immunolocalisation of Rab11a (a,e), E-cadherin (b,f), αV (c,g) and β3 (d,h) in the glandular epithelium of receptive phase endometrial samples (from women with proven fertility (a–d) and unexplained infertility (e–h) $n = 6$ each) at lower magnification. Panels (i-l) are the sections where the respective primary antibody was omitted.